ELSEVIER

Thermochimica Acta 267 (1995) 389–396

thermochimica acta

High temperature heat capacities and electrical conductivities of UO_2 doped with Nd and Mg[1]

Yuji Arita, Tsuneo Matsui*

Department of Nuclear Engineering, Faculty of Engineering, Nagoya University, Furo-cho, Chikusa-Ku, Nagoya 464-01, Japan

Received 1 November 1994; accepted 11 March 1995

Abstract

Heat capacities of $(U_{0.91}Nd_{0.09})O_2$, $(U_{0.91}Mg_{0.09})O_2$ and $(U_{0.85}Mg_{0.15})O_2$ were measured by direct heating pulse calorimetry over the temperature range from 300 to 1500 K. An anomalous increase in the heat capacity curve of these samples was observed above 1250, 1300 and 750 K, respectively, similar to those observed earlier in the cases of $(U_{1-y}M_y)O_2$ (where M = Gd, La, Sc, Eu and Y) by the present authors. Assuming the anomalous increase is due to the formation of Frenkel defects of oxygen, the enthalpy of defect formation was calculated from the excess heat capacity. However, no anomaly was seen in the electrical conductivity curve of these samples around the onset temperatures of the anomalous increase in the heat capacity curve, suggesting that the anomalous increase is not due to the formation of electron-hole pairs. The difference in the onset temperatures of UO_2 doped with various cations such as rare-earth elements and Mg was discussed in relation to the mean cation–oxygen interatomic distances which reflect the variety of the distribution of oxygens around the cations in the lattice, i.e. that of local structural environments for cation–oxygen bonding. The mean cation–oxygen interatomic distances were calculated from the ionic radii and the experimental lattice constants, assuming a perfect fluorite structure for these oxides. A linear relationship was found to exist between the onset temperature of the heat capacity anomaly and the difference in the mean cation–oxygen interatomic distance. The variety of local structures and defect clusters composed of Mg^{2+} and U^{5+} ions in UO_2 are thought to be related to the heat capacity anomaly.

Keywords: Heat capacity; Electrical conductivity; UO_2; Nd doped UO_2; Mg doped UO_2

* Corresponding author.

[1] Presented at the 30th Anniversary Conference of the Japan Society of Calorimetry and Thermal Analysis, Osaka, Japan, 31 October–2 November 1994.

SSDI 0040-6031 (95) 02496-4

1. Introduction

Heat capacities of $(U_{1-y}M_y)O_2$ (M = Gd [1], La [2], Eu [3], Y [4], Sc [5] and simulated fission-products [4,6]) have been measured over the temperature range from 300 to 1500 K by the present authors. An anomalous increase in the heat capacity curve of each doped UO_2 sample was observed to occur at temperatures ranging from about 550 to 1300 K depending on the dopant and its concentration. This anomalous increase was attributed to the formation of Frenkel pair-like defects of oxygen by the authors [1–6] as in the case of UO_2 [7–9]. However, there have been no data on the heat capacities of UO_2 doped with a divalent cation. Hence in the present study, the heat capacities and the electrical conductivities of UO_2 doped with Nd and Mg were measured over the temperature range from 300 to 1500 K by direct heating pulse calorimetry to investigate further the origin of the heat capacity anomaly in doped UO_2. The correlation between the variation in the onset temperatures of the heat capacity anomaly and the local structural arrangements of oxygen around the dopants in UO_2 is also discussed.

2. Experimental

2.2. Direct heating pulse calorimeter

The heat capacities and the electrical conductivities were measured simultaneously by using direct heating pulse calorimetry, described in detail previously [10]. In this calorimeter, a sample rod was first heated to a desired temperature by an external platinum heater. After attaining equilibrium conditions (constant desired temperature), an electric current was directly supplied to the sample rod for a short period (usually 1 s) through a regulated DC power supply and the temperature rise of the sample (generally 2–5 K) was measured by a Pt/Pt–13%Rh thermocouple. In this calorimeter, the sample rod was surrounded by double concentric cylindrical thermal shields made of molybdenum. In order to reduce the error in the measured heat capacity due to heat leak from the sample at high temperatures, the molybdenum shields were heated by using batteries in order to generate the same temperature rise in the shield as in the sample, i.e. to attain the adiabatic condition. The electric potential drop, the current and the temperature rise in the sample rod were measured to obtain the heat capacity and the electrical conductivity of the sample simultaneously. The heat capacity measurement was conducted within an error of ±2%, which was obtained by comparing the heat capacity of undoped UO_2 determined in this study with the previous literature values [1,4,11].

2.3. Sample preparation and characterization

The mixture of UO_2 and Nd_2O_3 or MgO, all of which are 99.99% pure, was shaped into a cylindrical rod of about 6–7 mm in diameter and about 50–70 mm in length, using an evacuated rubber press under a hydrostatic pressure of about 400 MPa. The cylindrical rod of UO_2 doped with Nd_2O_3 was homogenized and sintered by heating at 1673 K for 7 days in an Ar gas flow, and then at 1273 K for 2 days in a hydrogen gas flow to obtain

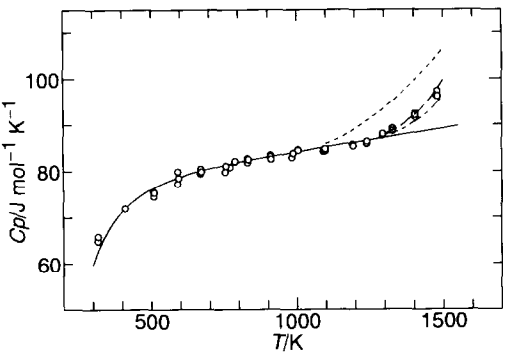

Fig. 1. Temperature dependence of the heat capacity of $(U_{0.910}Nd_{0.090})O_2$; O, $(U_{0.910}Nd_{0.090})O_2$ in this study; ——, undoped UO_2 [1,4]; ------, $(U_{0.910}La_{0.090})O_2$ [2], – – – –, $(U_{0.910}Sc_{0.090})O_2$[5], - - - -, $(U_{0.910}Y_{0.090})O_2$ [4].

the stoichiometric composition of oxygen (O/(M + U) = 2.00) according to a thermogravimetric study [12]. The cylindrical rods of UO_2 doped with 9 at.% and 15 at.% MgO were prepared at 1673 K for 7 days in a purified Ar gas flow and in an Ar gas flow, respectively, in order to obtain the stoichiometric composition of oxygen (O/(M + U) = 2.00) according to the thermogravimetric studies for both samples [13,14]. The homogenizing and sintering processes were repeated several times. X-Ray diffraction analysis indicated the presence of a single fluorite phase for each sample.

3. Results and discussion

The heat capacities of UO_2 doped with Nd and Mg measured in this study are shown in Figs. 1 and 2, respectively, together with the literature data for undoped [1,4] and

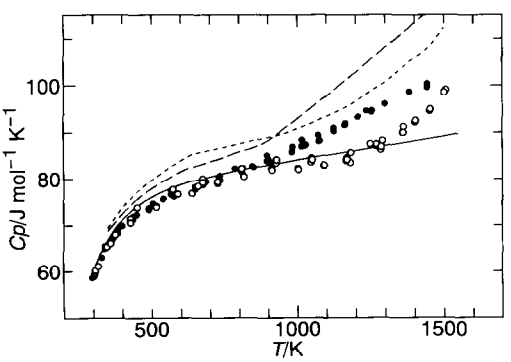

Fig. 2. Temperature dependences of the heat capacities of $(U_{1-y}Mg_y)O_2$ ($y = 0.090$ and 0.150). O, $(U_{0.910}Mg_{0.090})O_2$; ●, $(U_{0.850}Mg_{0.150})O_2$ in this study; ——, undoped UO_2 [1,4]; ------, $(U_{0.858}La_{0.142})O_2$ [2], – – – –, $(U_{0.858}Gd_{0.142})O_2$ [1].

doped UO_2 [1,2,4,5]. An anomalous increase in the heat capacity curve of $(U_{0.91}Nd_{0.09})O_2$, $(U_{0.91}Mg_{0.09})O_2$ and $(U_{0.85}Mg_{0.15})O_2$ is seen above 1250, 1300 and 750 K, respectively, similar to that observed in the case of UO_2 doped with Gd [1], La [2], Y [4] and Sc [5]. It is seen from the figure that the onset temperatures of the heat capacity anomalies of UO_2 doped with various cations are different even when the dopant concentrations are the same.

The excess heat capacity was evaluated by subtracting the smoothed base line of the heat capacity from the experimental values for the temperatures above the onset temperature. The smoothed base line was determined by applying a least-squares fitting for the data in the temperature range below the onset temperature and then extrapolating the fitted line to the range above the onset temperature. Assuming that the excess heat capacity is due to the formation of Frenkel pairs of oxygen, as in the cases of UO_2 doped with Gd [1], La [2], Y [4] and Sc [5], the excess heat capacity ΔC can be expressed as [8]

$$\Delta C = \{(\Delta H_f)^2/(\sqrt{2}\,RT^2)\} \exp(\Delta S_f/2R) \exp(-\Delta H_f/2RT) \quad (1)$$

where ΔS_f and ΔH_f are the entropy and enthalpy of formation of a Frenkel-pair, respectively. The enthalpies of formation for a Frenkel-pair in $(U_{0.01}Nd_{0.09})O_2$, $(U_{0.91}Mg_{0.09})O_2$ and $(U_{0.95}Mg_{0.15})O_2$ obtained from Eq. (1) in this study are shown in Fig. 3 together with those of UO_2 [8] and $(U_{1-y}M_y)O_2$ (M = Gd, La, Sc, Eu and Y) reported previously [1–6]. It is seen that the enthalpies for $(U_{1-y}M_y)O_2$ (M = Nd and Mg) are slightly larger than those for UO_2 doped with trivalent cations (except Sc) for the same dopant concentrations. Also, their dependence on the concentration of the dopant was found to be different from that observed for UO_2 doped with Gd, La, Eu and Y. However, the enthalpies for $y = 0$ obtained by the extrapolation of both curves are not so different from the value for

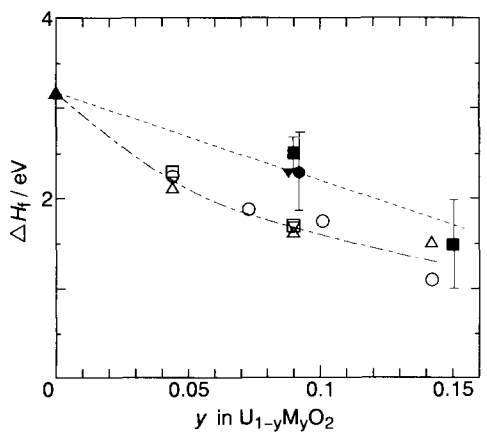

Fig. 3. Enthalpy of defect formation. ◆, $(U_{0.910}Nd_{0.090})O_2$ and ◇, $(U_{1-y}Mg_y)O_2$ with error bar in this study; ▲, UO_2 [8], O, $(U_{1-y}Gd_y)O_2$ [1]; ▽, $(U_{1-y}La_y)O_2$ [2]; ●, $(U_{1-y}Eu_y)O_2$ [3]; □, $(U_{0.910}Sc_{0.090})O_2$ [5]; ■, $(U_{0.910}Y_{0.090})O_2$ [4].

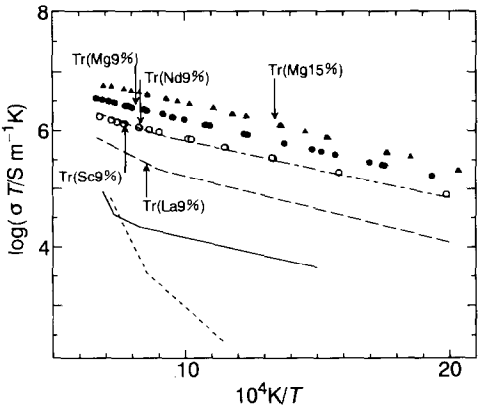

Fig. 4. Electrical conductivity of $(U_{1-y}M_y)O_2$ O, $(U_{0.910}Nd_{0.090})O_2$; ●, $(U_{0.910}Mg_{0.090})O_2$ and ▲, $(U_{0.850}Mg_{0.150})O_2$ in this study; ——, undoped UO_2 [15]; ------, $(U_{0.990}Nb_{0.010})O_2$ [5], – – – –, $(U_{0.10}La_{0.090})O_2$ [2], - - - -, $(U_{0.910}Sc_{0.090})O_2$ [5].

undoped UO_2, showing that the heat capacity anomaly of these doped samples has the same origin as that of undoped UO_2. The difference between the enthalpy of defect formation for UO_2 doped with Mg (or Sc) and that for UO_2 doped with other trivalent cations is discussed later in this paper in relation to the local structural environment.

The electrical conductivities of $(U_{0.91}Nd_{0.09})O_2$, $(U_{0.91}Mg_{0.09})O_2$ and $(U_{0.95}Mg_{0.15})O_2$ were also measured and the results are shown in Fig. 4 together with those for undoped UO_2 [15] and UO_2 doped with other cations [2,5], where the onset temperatures of the anomalous increase in the heat capacity are shown by the vertical arrows. No significant change of slope is seen in the electrical conductivity curve of each sample of $(U_{0.91}Nd_{0.09})O_2$, $(U_{0.91}Mg_{0.09})O_2$ and $(U_{0.95}Mg_{0.15})O_2$ at the temperatures where the heat capacity starts increasing anomalously. Although the increase in the slope is observed for some doped UO_2 samples such as $(U_{0.91}La_{0.09})O_2$, and $(U_{0.99}Nb_{0.01})O_2$ in Fig. 4, the increase in the slope is thought to be due to the gradual transition from the extrinsic to the intrinsic conduction region from the following facts. (1) The temperature at which the slope of the conductivity changes is almost independent of the dopant and its concentration, and is close to that of undoped UO_2. (2) The temperature at which the slope changes does not always coincide with the onset temperature of the heat capacity anomaly. (3) The increase of the slope in the conductivity curve is also observed in $(U_{0.99}Nb_{0.01})O_2$, which showed no heat capacity anomaly. Therefore, the excess heat capacity of $(U_{0.91}Nd_{0.09})O_2$, $(U_{0.91}Mg_{0.09})O_2$ and $(U_{0.95}Mg_{0.15})O_2$ is not likely due to the formation of electron-hole pairs.

The local structural environments of Y^{3+} and Zr^{4+} ions in 18 wt.% Y_2O_3 doped ZrO_2 were previously studied by using extended X-ray absorption fine structure spectroscopy (EXAFS) over the temperature range from 153 to 1043 K [16]. The oxygen arrangement around Y^{3+} and Zr^{4+} was found to be different from each other, i.e. more oxygen vacancies were adjacent to Zr^{4+} than Y^{3+} and those near Zr^{4+} were more disordered than those near Y^{3+} at low temperatures.

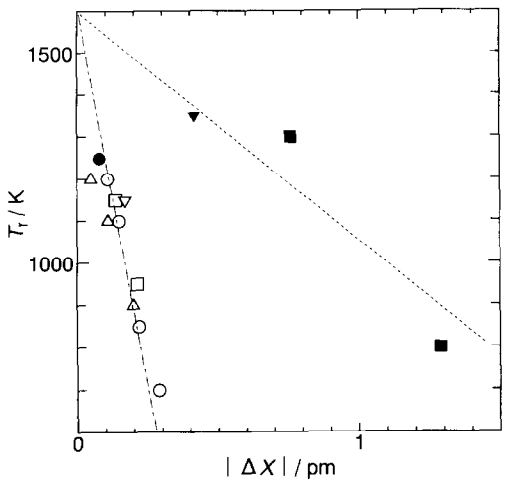

Fig. 5. Relation between the onset temperature of the heat capacity anomaly and the value of Δx for doped UO_2 in Eq. (2). ●, $(U_{0.910}Nd_{0.090})O_2$ and ■, $(U_{1-y}Mg_y)O_2$ in this study; ○, $(U_{1-y}Gd_y)O_2$ [1], △, $(U_{1-y}La_y)O_2$ [2]; □, $(U_{1-y}Eu_y)O_2$ [3]; ▼, $(U_{0.910}Sc_{0.090})O_2$ [5]; ▽, $(U_{0.910}Y_{0.090})O_2$ [4]; -----, for Mg^{2+} and Sc^{3+} ($\Delta x < 0$); – – – –, for other trivalent cations ($\Delta x > 0$).

The structural environment of Zr^{4+} in cubic ZrO_2 resembled that of the 7-coordinated Zr^{4+} in monoclinic ZrO_2. Increasing the temperature of the sample resulted in the local structural environments of the two cations becoming more alike, suggesting that increased oxygen mobility leads to an increasing random distribution of oxygen defects. Therefore, similar to the case of ZrO_2, the oxygen arrangement around M^{3+} and M^{2+} dopants in UO_2, that is the same fluorite structure as ZrO_2, is expected to be different from that around U ions. It is also expected that, with increasing temperature, increased oxygen mobility will make the distribution of oxygen defects around M^{2+}, M^{3+}, U^{4+} and U^{5+} uniform (disorder), resulting in the heat capacity anomaly.

In Fig. 5 the onset temperatures of the heat capacity anomaly of UO_2 doped with Nd and Mg cations are plotted against $|\Delta x|$ along with our previous results on UO_2 doped with various trivalent cations [1–3,6]. The value of Δx is calculated from the following equation [17]:

$$\Delta x = \{(r_c + r_o) - \sqrt{3}/4a_1\}_A - \{(r_u + r_o) - \sqrt{3}/4a_2\}_B \quad (2)$$

where A and B represent the values in doped UO_2 and undoped UO_2, respectively. In the above equation r_c, r_o and r_u represent the mean ionic radius of all the cations (M^{2+}, M^{3+}, U^{4+} and U^{5+}) with eightfold coordination in doped UO_2, the ionic radius of an oxygen ion with fourfold coordination and the ionic radius of a uranium ion with eightfold coordination, respectively, and the values for these terms reported by Shannon [18] were used in the present calculations. The literature data [13,19–24] for the lattice constants of doped UO_2 (a_1) and undoped UO_2 (a_2) determined experimentally were employed in the calculation. As can be seen from Fig. 5, the onset temperatures (T_r) of the anomalous increase

in heat capacity curve for all the doped UO_2 were found to decrease linearly with increasing $|\Delta x|$. This indicates that the larger is the change in the mean cation–oxygen interatomic distance (i.e. the more complex the distribution of oxygen defects) caused by the introduction of an aliovalent cation, the lower becomes the onset temperature. Further, the values for all the doped UO_2 with the exception of Mg and Sc, fall on the same straight line irrespective of the dopant and its concentration. In the case of UO_2 doped with Mg and Sc, their onset temperatures plotted as a function of $|\Delta x|$ falls on a different straight line, as shown in Fig. 5. Since the $|\Delta x|$ for UO_2 doped with Mg was also calculated by adopting the same procedure as for the trivalent cations, the complexity of the arrangement of oxygen atoms around the trivalent cation could not be sufficiently expressed by $|\Delta x|$ alone. This different dependence of the onset temperatures on Δx due to the formation of cation defect clusters composed of Mg^{2+} (or Sc^{3+}) and U^{5+}, since (1) the ionic radii of Mg^{2+} and Sc^{2+} are smaller than that of U^{4+}, different from other trivalent cations, i.e. $\Delta x < 0$ for Mg^{2+} and Sc^{3+}, different from $\Delta x > 0$ for other cations, and (2) the presence of the formation of cation defect clusters (Mg^{2+}–U^{5+}) has been proposed in the discussion of the oxygen potential of $(U_{1-y}Mg_y)O_2$ [25]. Slightly higher values of the enthalpies of formation for a Frenkel-pair of oxygen in $(U_{1-y}Mg_y)O_2$ (M = Mg and Sc) are thought to originate from the formation of such metal clusters.

To clarify the validity of the present discussion, the precise structural analysis by EXAFS is now in progress in our laboratory.

4. Conclusions

The conclusions obtained in this study are summarized as follows: (1) for each sample of $(U_{0.91}Nd_{0.09})O_2$, $(U_{0.91}Mg_{0.09})O_2$ and $(U_{0.95}Mg_{0.15})O_2$, an anomalous increase in the heat capacity was observed above 1250, 1300 and 750 K, respectively, as was previously observed in the cases of $(U_{1-y}M_y)O_2$ (M = Gd, La, Y, Eu and Sc) by the present authors. (2) The enthalpies of formation for oxygen Frenkel defects were calculated from the excess heat capacity of $(U_{0.91}Nd_{0.09})O_2$, $(U_{0.91}Mg_{0.09})O_2$ and $(U_{0.95}Mg_{0.15})O_2$. The value obtained by extrapolating the enthalpy values of doped UO_2 to zero dopant concentration of the dopant is in agreement with that of undoped UO_2. (3) The excess heat capacity is thought to be due to the predominant formation of Frenkel defects of oxygen. (4) The onset temperatures of the heat capacity anomaly observed for Gd, La, Y, Eu, Sc, Nd and Mg-doped UO_2, decreased linearly with increasing $|\Delta x|$ values, the difference between the mean cation–oxygen interatomic distance in the doped and undoped UO_2 which was calculated from the ionic radii of the dopants and U host ion as well as the lattice constants. Since the Δx thus obtained is thought to be related to the degree of complexity of the distribution of oxygen defects around the cations in the UO_2 lattice, i.e. that of the local structural environments for cation–oxygen bonding, the larger the Δx will be, the easier the formation of oxygen defects, and, hence lower will be the onset temperature of the heat capacity anomaly. (5) The reason for the difference in the dependence of the onset temperatures on $|\Delta x|$ for UO_2 doped with Mg and Sc from that of UO_2 doped with other trivalent cations has not been fully understood. The main reason for the difference is believed to be the ionic radii of $Mg^{2+}$and Sc^{3+} being smaller than that of U^{4+},

unlike other trivalent cations and may be related to the formation of the defect clusters composed of Mg^{2+} (or Sc^{2+}) and U^{5+}.

References

[1] H. Inaba, K. Naito and M. Oguma, J. Nucl. Mater., 149 (1987) 341.
[2] T. Matsui, Y. Arita and K. Naito, J. Radioanal. Nucl. Chem., 143 (1991) 149.
[3] T. Matsui, T. Kawase and K. Naito, J. Nucl. Mater., 186 (1992) 254.
[4] T. Matsui, Y. Arita and K. Naito, J. Nucl. Mater., 188 (1992) 205.
[5] T. Matsui, Y. Arita and K. Naito, Solid State Ionics, 49 (1991) 195.
[6] Y. Arita, S. Hamada and T. Matsui, Thermochim. Acta, 247 (1994) 225.
[7] J.F. Kerrisk and D.C. Clifton, Nucl. Technol., 16 (1972) 531.
[8] R. Szwarc, J. Phys. Chem. Solids, 30 (1969) 705.
[9] P. Browning, J. Nucl. Mater., 98 (1981) 345.
[10] K. Naito, H. Inaba, M. Ishida and K. Seta, J. Phys., E12 (1979) 712.
[11] F. Grønvold, N.J. Kveseth, A. Sveen and J. Tichy, J. Chem. Thermodyn., 2 (1970) 665.
[12] K. Une and M. Oguma, J. Nucl. Mater., 118 (1983) 189.
[13] T. Fujino and K. Naito, J. Inorg. Nucl. Chem., 32 (1970) 627.
[14] T. Fujino, J. Tateno and J. Tagawa, J. Solid State Chem., 24 (1978) 11.
[15] T. Matsui and K. Naito, J. Nucl. Mater., 138 (1986) 19.
[16] C.R.A. Catlow, A.V. Chadwick, O.N. Greaves and L.M. Moroney, J. Am. Ceram. Soc. 69 (1986) 272.
[17] Y. Arita, T. Matsui and S. Hamada, Thermochimica Acta, 253 (1995) 1.
[18] R.D. Shannon, Acta Crystallogr., A32 (1976) 751.
[19] S. Aronson and J.C. Clayton, J. Chem. Phys., 35 (1961) 1055.
[20] W.A. Young, L. Lynds and J.S. Mohi , NAA-SR-6765 (1962).
[21] T. Ohmichi, S. Fukushima, H. Tagawa and H. Watanabe, J. Nucl. Mater., 105 (1981) 40.
[22] D.I.R. Norris and P. Kay, J. Nucl. Mater., 116 (1983) 184.
[23] K. Une and M. Oguma, J. Nucl. Sci. Technol., 20 (1983) 844.
[24] T. Fujino, J. Inorg. Nucl. Chem., 34 (1972) 1563.
[25] T. Fujino and N. Sato, J. Nucl. Mater., 189 (1992) 103.